

# DCXR promotes cell proliferation by promoting the activity of aerobic glycolysis in breast cancer

YONGMEI JIN<sup>1\*</sup>, MIAO ZHANG<sup>2\*</sup>, YANG TONG<sup>1</sup>, LIN QIU<sup>1</sup>, YING YE<sup>2</sup> and BIN ZHAO<sup>1</sup>

<sup>1</sup>Department of General Surgery; <sup>2</sup>Central Laboratory, The Seventh People's Hospital of Shanghai University of Traditional Chinese Medicine, Shanghai 200137, P.R. China

Received April 2, 2022; Accepted September 13, 2022

DOI: 10.3892/mmr.2022.12918

**Abstract.** The function of human dicarbonyl/L-xylulose reductase (DCXR) in the pathophysiology of breast cancer is yet to be elucidated. The present study aimed to investigate the function of DCXR in glycolysis and the cell cycle of breast cancer cells with respect to cell proliferation. Differential expressed DCXR was identified in The Cancer Genome Atlas (TCGA) database and verified in clinical breast cancer tissue. DCXR silencing and overexpression were induced by RNA interference and lentiviral vectors, respectively. Cell cycle progression, proliferation and glycolytic activity of breast cancer cells were detected by flow cytometry, Cell Counting Kit-8 assay and chemical methods, respectively. Tumorigenicity was detected using nude mice xenograft models. The expression of DCXR was increased in TCGA breast cancer database and the function of DCXR was enriched in 'glycolysis' and 'cell cycle'. Further analysis using clinical breast cancer samples confirmed upregulation of DCXR. The silencing of DCXR suppressed proliferation and cell cycle progression of breast cancer cells and significantly decreased the capacity for glycolysis, thereby demonstrating the effect of DCXR on the function of breast cancer cells. Similar conclusions were obtained in DCXR overexpressing cells; notably, DCXR overexpression promoted proliferation, cell cycle progression at S phase and glycolysis. 2-Deoxy-D-glucose inhibited the effect of DCXR on the proliferation and cell cycle progression

of breast cancer cells. The present study revealed that DCXR regulated breast cancer cell cycle progression and proliferation by increasing glycolysis activity and thus may serve as an oncogene for breast cancer.

## Introduction

Breast cancer surpassed lung cancer as the most commonly diagnosed cancer in 2020, with an estimated 2.3 million new cases, representing 11.7% of all cancer cases; in addition, it is the fifth leading cause of cancer mortality worldwide, with 685,000 deaths (1). Breast cancer is a life-threatening malignant tumor, which is the major cause of premature death in women (2). Despite advances in the diagnosis, drug development and personalized treatment based on molecular classification of breast cancer (3,4), diagnostic markers and therapeutic targets are still lacking. Therefore basic research on this topic is a hotspot (5,6). Elucidating the function of metabolism-associated proteins in regulating breast cancer cell metabolism is a promising prospect for identifying diagnostic and therapeutic targets for breast cancer (7).

Cancer cells alter their metabolism to promote survival, proliferation and long-term maintenance. The common features of this altered metabolism include increased glucose uptake and fermentation of glucose to lactate. This phenomenon is observed even in the presence of completely functioning mitochondria and is known as 'the Warburg effect' (8). Cancer cells use glycolysis as the primary energy source for proliferation and cell cycle progression, which is different from normal cells that rely on oxidative phosphorylation in the mitochondria for energy (9). Although this phenomenon is elusive, accumulating evidence since Warburg reported that cancer cells metabolize glucose in the 1920s (10), has supported the hypothesis that glycolysis is the primary energy metabolism method used to meet the needs of cancer cells for continuous cell proliferation (9,11). Furthermore, aerobic glycolysis supports tumor progression, particularly in breast cancer cells (8). Previous studies have reported that glycolysis affects the proliferation and progression of breast cancer (12-14). However, the regulatory mechanism of aerobic glycolysis in breast cancer cells is unknown.

Dicarbonyl/L-xylulose reductase (DCXR) is a highly conserved enzyme in mammals that catalyzes conversion of L-xylulose into xylitol (15). The role of DCXR in L-xylulose

*Correspondence to:* Professor Ying Ye, Central Laboratory, The Seventh People's Hospital of Shanghai University of Traditional Chinese Medicine, 358 Datong Road, Pudong, Shanghai 200137, P.R. China  
E-mail: yy49453324@163.com

Professor Bin Zhao, Department of General Surgery, The Seventh People's Hospital of Shanghai University of Traditional Chinese Medicine, 358 Datong Road, Pudong, Shanghai 200137, P.R. China  
E-mail: zhao66@sina.cn

\*Contributed equally

**Key words:** dicarbonyl/L-xylulose reductase, breast cancer, glycolysis, cell cycle, proliferation

metabolism has been known for decades (16); however, the role of DCXR in normal human physiology and pathophysiology remains to be elucidated. Previous studies have shown that DCXR expression disorder is observed in age- and metabolism-associated diseases, especially in human male infertility, nephropathy and diabetes (17). DCXR has multi-functional properties with respect to carbonyl reductase and non-catalytic function (18). Previous studies have linked the role of DCXR with cell adhesion, indicating its novel role in tumor progression and metastasis (18,19). Moreover, certain studies have reported that DCXR is abnormally expressed in cancer tissue; for example, DCXR is overexpressed in prostate adenocarcinoma and melanoma (20-22) and downregulated in hepatocellular carcinoma (23). Furthermore, these studies reported a correlation between abnormal DCXR expression levels and cancer progression or poor prognosis but did not determine the role of the protein. The correlation between DCXR and cancer is a promising research subject; therefore, the protein function needs to be assessed further. To the best of our knowledge, only a few studies have reported the expression of DCXR in breast cancer tissue (18,24); however, the effect of this protein on the pathological mechanisms of cancer progression has not yet been assessed.

The present study evaluated the DCXR expression pattern in breast cancer tissue by assessing breast cancer databases and clinical tissue samples. Further functional analysis focused on the role of DCXR in glycolysis, cell cycle and proliferation using DCXR-overexpression and -silencing in breast cancer cell lines. The assessment of the function and pathological mechanism of DCXR may demonstrate DCXR to be a candidate for cancer molecular targeting therapy in breast cancer.

## Materials and methods

**Bioinformatics analysis.** DCXR expression data and survival data from patients with breast cancer [paracancerous (n=113) and tumor (n=1,104) tissue data] were obtained from The Cancer Genome Atlas (TCGA) databases (<https://tcga-data.nci.nih.gov/tcga/>). Gene set enrichment analysis (GSEA) was performed by the JAVA program (<http://www.broadinstitute.org/gsea>) using MSigDB portal. Enrichment Score (ES) was calculated via the Kolmogorov-Smirnov test and the calculation of ES significance level was analyzed by permutation test; finally, the false discovery rate method was used for multiple hypothesis testing correction, and  $\log_2$ fold-change $>1$  and  $P<0.05$  were set as the cut-off for enrichment.

**Human samples.** A total of 80 pairs of paracancerous and cancer tissue samples (1 cm distance) were obtained from patients (mean age, 49 years; age range, 30-70 years) who underwent breast tumor resection surgery at Seventh People's Hospital of Shanghai University of Traditional Chinese Medicine (Shanghai, China) between September 2020 and August 2021. Patients who received chemotherapy or radiation prior to resection were excluded from the present study. Resected tissues were stored at  $-80^{\circ}\text{C}$  until examination. All patients provided written informed consent. Tissue DCXR mRNA and protein expression levels were assessed using reverse transcription-quantitative PCR (RT-qPCR) and

immunohistochemistry. Protocols using human samples were approved by the Independent Ethics Committee of The Shanghai Seventh People's Hospital (approval no. 2020-7th-H IRB-031) and followed the Declaration of Helsinki.

**Cell culture.** MDA-MB-231, BT-474, T47D, MCF-7 and ZR751 human breast cancer cell lines were purchased from the The Cell Bank of Type Culture Collection of The Chinese Academy of Sciences. MCF-10A human normal mammary epithelium cell line (Procell Life Science & Technology Co., Ltd.) was used as the control. Cells were grown in DMEM (Thermo Fisher Scientific, Inc.), with 10% fetal calf serum (Thermo Fisher Scientific, Inc.), L-glutamine (2 mM) and 1% penicillin/streptomycin (Beijing Solarbio Science & Technology Co., Ltd.). All cells were cultured with 5%  $\text{CO}_2$  at  $37^{\circ}\text{C}$ .

**RT-qPCR.** From the 80 patients, a total of 30 pairs of paracancerous and cancer tissue samples were randomly selected. Tissue and cell DCXR mRNA expression levels were assessed by RT-PCR. Total RNA was extracted from BT-474, ZR751, MCF-7, MDA-MB-231, T47D and MCF-10A cells, and human breast cancer and adjacent tissues using TRIzol® (Invitrogen; Thermo Fisher Scientific, Inc.). After determination of purity and quality, RT was performed using Maxima SYBR Green/ROX Qpcr Pre-mixed solution (2X) (cat. no. K0233; Thermo Fisher Scientific, Inc.) at  $42^{\circ}\text{C}$  for 1 h, followed by  $70^{\circ}\text{C}$  for 15 min. The Cdna product was used for Qpcr with the following thermocycling conditions: Initial denaturation of  $95^{\circ}\text{C}$  for 10 min; followed by 40 cycles of  $95^{\circ}\text{C}$  for 15 sec and  $60^{\circ}\text{C}$  for 45 sec (Takara Biotechnology Co., Ltd.). The primers were as follows: DCXR forward, 5'-GAATGTCTCCAGCCA GTG-3' and reverse, 5'-GGATTTCGGTTCAGCATAG-3'; GAPDH forward, 5'-CAAATTCATGGCACCCTCA-3' and reverse, 5'-GCATCGCCCCACTTGATTTT-3'. GAPDH was used as an internal control. Relative DCXR Mrna expression levels were calculated using the  $2^{-\Delta\Delta\text{Ct}}$  method in three replicate experiments (25).

**Western blotting.** From the 80 patients, a total of 30 pairs of paracancerous and cancer tissue samples were randomly selected. Tissue and cell DCXR protein expression levels were assessed by western blotting. Total proteins were extracted from MDA-MB-231, BT-474, T47D, MCF-7 and ZR751 human breast cancer cell lines using RIPA lysis buffer (Thermo Fisher Scientific, Inc.). The protease inhibitor (Thermo Fisher Scientific, Inc.) was pre-dissolved in the lysis buffer to prevent proteolysis. The obtained protein samples underwent quantitative analysis with an enhanced BCA protein assay kit (Thermo Fisher Scientific, Inc.) and stored at  $-20^{\circ}\text{C}$  until subsequent experimentation. A mixture of loading buffer with an equal amount of protein samples (25  $\mu\text{g}$ ) was loaded onto 10% SDS-PAGE to separate proteins of different molecular weights. Protein was then transferred to nitrocellulose membranes (MilliporeSigma). Non-specific protein on the membrane was blocked using 5% non-fat dried milk dissolved in 1X PBS containing 0.05% Tween-20 for 1 h at room temperature. The membranes were then incubated with the blocking buffer-diluted primary antibodies overnight at  $4^{\circ}\text{C}$ . The primary antibodies used are as follows: DCXR

(1:1,000; cat. no. ab110283; Abcam) and  $\beta$ -actin (1:2,000; cat. no. 4970; Cell Signaling Technologies, Inc.). After rinsing with Tris-HCl buffer (pH 7.4, 20 mM), membranes were incubated at room temperature with the corresponding secondary antibodies bound to horseradish peroxidase (anti-rabbit, 1:2,000, cat. no. A0208; anti-mouse, 1:2,000, cat. no. A0216; both from Beyotime Institute of Biotechnology) for 2 h. The probed targeted proteins were visualized using a Tanon-5200 Multi-Imaging System (Tanon Science and Technology Co., Ltd.) following treatment with an Tanon™ ECL chemiluminescence substrate kit (cat. no. 180-501; Tanon Science and Technology Co., Ltd.). The relative protein levels were semi-quantified using ImageJ V1.8.0 software (National Institutes of Health).

**DCXR knockdown and overexpression vector construction and transduction into breast cancer cells.** Three short hairpin (sh)RNAs targeting three different human DCXR gene loci were synthesized (shDCXR-1, shDCXR-2 and shDCXR-3). The shRNA sequences were: shDCXR-1, 5'-CACCGGCCTTTGACAGATCCTTTGACGAATCAAAGGATCTGTCAAAGGCC-3'; shDCXR-2, 5'-CACCGCGGGCAGTAACCTAACCATAGCGAACTATGGTTAGTTACTGCCCGC-3'; shDCXR-3, 5'-CACCGAATCCCACTTGGCAAGTTTGCGAACAAACCTTGCCAAGTGGGATTC-3'. A scrambled sequence was used as shRNA negative control (shNC). shDCXR and shNC were constructed in lentiviral plasmids (pLKO.1) using a 2nd generation system and 293T cells (The Cell Bank of Type Culture Collection of The Chinese Academy of Sciences) were transfected with these plasmids to produce lentiviruses using Lipofectamine® 2000 (Invitrogen; Thermo Fisher Scientific, Inc.); the ratio of plasmids, pMD2.G and psPAX2 (Shanghai GenePharma Co., Ltd.) was 2:1:2. All shRNAs were purchased from Shanghai Majorbio Bio-Pharm Technology Co., Ltd. For overexpression of DCXR in the breast cancer cell lines, recombinant overexpression DCXR (oeDCXR) was generated using the pLVX-puro lentiviral plasmid constructed with DCXR (NM\_016286.4) cDNA (2nd generation system). An empty plasmid was used as oeNC. The overexpression lentiviral plasmids were generated in 293T cells according to the aforementioned protocol for shDCXR and shNC. oeDCXR and oeNC were purchased from Shanghai GenePharma Co., Ltd. The quantity of lentiviral plasmid used for transfection was 5  $\mu$ g ( $10^8$  TU/ml). For breast cancer transduction, MDA-MB-231 cells were seeded in a 24-well plate and cultured to 70-80% confluency at 37°. shDCXRs or oeDCXR were added in the presence of Lipofectamine 2000 (26). The concentration of purinomycin used for screening was 7  $\mu$ g/ml, and after 48 h transduction at 37°C, the cells were harvested for analysis.

**Cell Counting Kit-8 (CCK-8) assay for cell proliferation.** Cell proliferation was evaluated using CCK-8 assay (Signalway Antibody LLC). Briefly, followed by treatment with shRNA at 0, 12, 24 or 48 h transduction, cells were incubated with CCK-8 solution (1:10) for 1 h and the absorbance was measured at 450 nm using a microplate reader (BioTek Corporation).

**Flow cytometry.** Changes to the cell cycle were evaluated using propidium iodide (PI) staining on a flow cytometer

(Accuri C6; BD Biosciences). ZR751 and BT-474 cells ( $1 \times 10^6$ ) were suspended in PBS and fixed with 70% ethanol for 2 h at 20°C. RNase A (Beijing Solarbio Science & Technology Co., Ltd.) was used to treat cells for 15 min at 37°C. Cells were stained using PI (7Sea PharmTech Co., Ltd.) for 30 min in the dark at 4°C. The DNA content of each sample was analyzed by flow cytometry. The percentage of cells at G0/G1, S and G2/M phase was calculated using FlowJo v10.8 (FlowJo LLC).

**Chemical detection of ATP and lactate dehydrogenase (LD).** Cell ATP levels were assessed using a luciferase-based ATP assay kit (Beyotime Institute of Biotechnology) according to the manufacturer's protocol. Briefly, breast cancer cells were transduced with or without shRNA, the cells were scraped off with a cell scraper, and cell precipitates were collected by centrifugation at 272 x g for 10 min at room temperature. Subsequently, the cell precipitates were added to the lysis buffer of the ATP assay kit at a ratio of 50-100  $\mu$ l of lysis buffer to each well of a 24-well plate. The samples were then vortexed, after which, they were centrifuged at 12,000 x g for 5 min at 4°C, and the supernatant was obtained for subsequent determination. In 24-well plates, 100  $\mu$ l ATP detection reagent was added to 100  $\mu$ l supernatant at room temperature for 5 min. Luminescence was measured using a Safire II monochromator microplate reader (Tecan Group Ltd.). Standard curves were obtained by diluting standards using ATP diluents. The concentration of ATP in each sample was calculated from the standard curve. In order to eliminate the error caused by the difference in protein amount in sample preparation, the protein concentration of each treatment group was assessed using Bradford Protein Assay.

LD levels were assessed using breast cancer cells at the logarithmic growth stage transduced with shRNA or overexpression lentiviral particles; the blank control group was cultured the same way. The supernatant was collected by centrifugation at 12,000 x g for 5 min and diluted with 400  $\mu$ l normal saline at room temperature. The assay was performed according to the manufacturer's protocol (Lactic Acid assay kit; Nanjing Jiancheng Bioengineering Institute), heated in a 37°C water bath for 10 min and stop solution was then added. After mixing, the absorbance was measured at 530 nm (ELx800™; BioTek Corporation).

**Glycolysis and mitochondrial respiration assay.** MDA-MB-231 cells ( $5 \times 10^5$ /well) were cultured in 24-well plates. The extracellular acidification rate (ECAR) assay was used to evaluate glycolysis. Briefly, cells were grown in XF base medium (cat. no. 103575; Seahorse Bioscience; Agilent Technologies, Inc.) supplemented with 2 mM L-glutamine and 25 mM glucose. Glycolysis inhibitor 2-deoxy-D-glucose (2-DG; 10 mmol/l; Beijing Solarbio Science & Technology Co., Ltd.) and oligomycin (1  $\mu$ M; Beijing Solarbio Science & Technology Co., Ltd.) were used to treat cells at 37°C for 1 h to suppress glycolytic metabolism and the effects on breast cancer cells were assessed. For oxygen consumption rate (OCR) assay, cells were cultured in XF base medium with 1.0 oligomycin, 0.5 FCCP (a potent uncoupler of mitochondrial oxidative phosphorylation) and 0.45  $\mu$ M rotenone/antimycin A to assess mitochondrial oxidative phosphorylation. ECAR and OCR examination were performed using an XF24

Extracellular Flux Analyzer (Seahorse Bioscience; Agilent Technologies, Inc.).

**Immunohistochemistry (IHC) and fluorescence staining.** Human tissues were embedded in paraffin after fixing with 10% formalin at 4°C for 24 h. The sections (2  $\mu$ m) were dewaxed and rehydrated before IHC staining. Subsequently, the slides were soaked in 3% hydrogen peroxide solution for 15 min at room temperature to quench the endogenous peroxidase activity. To avoid producing non-specific binding, 2.5% goat serum (cat. no. ab7481; Abcam) was used to block the sections at room temperature for 1 h. A primary antibody against DCXR (1:500, cat. no. ab110283; Abcam) was used to incubate the sections at room temperature for 1 h, followed by incubation with the secondary antibodies (1:2,000; anti-mouse; cat. no. ab205719; Abcam) at room temperature for 30 min, and washing with TBS. Immunoreactivity was visualized using DAB and hematoxylin was used for counterstaining at room temperature for 1 min. Protein expression levels were assessed using a light microscope (ECLIPSE E100; Nikon Corporation) and imaged. For IHC, the scoring system was composed of staining intensity (A) and positive areas (B). A was scored as no staining (0), weak staining (1+), moderate staining (2+) or strong staining (3+). B was classified as 0% (0+), 1-10% (1+), 11-25% (2+), 26-50% (3+) or 51-100% (4+). The total score of A and B was 0-9 for each specimen; 0-3 was defined as low protein expression and 4-9 defined as high protein expression of DCXR.

For fluorescence staining, tissue samples were fixed with 4% paraformaldehyde at room temperature for 24 h, embedded in paraffin and cut into 2- $\mu$ m sections. Subsequently, the sections were dewaxed with xylene for 15 min and rehydrated conventionally using an ethanol gradient (from 99 to 70%, followed by demineralized water). The endogenous peroxidase activity was blocked at room temperature using 3% hydrogen peroxide solution for 15 min. After blocking the non-specific protein binding with 5% skimmed milk at room temperature for 30 min, sections were incubated with anti-Ki67 antibody (1:500; cat. no. ab15580; Abcam) at 4°C overnight. Following incubation with Alexa Fluor 488-labeled goat anti-mouse IgG antibody (1:500; cat. no. A0428; Beyotime Institute of Biotechnology) for 1 h at room temperature. Images of the stained sections were captured using a ZEISS fluorescence microscope (Zeiss AG).

**Xenograft model in nude mice.** The study protocol for animal experimentation was approved by the Ethics Committee of Shanghai Seventh People's Hospital (approval no. 2021-AR-011) and conformed to the ethical guidelines of the National Institutes of Health Guide for the Care and Use of Laboratory Animals (NIH Publications No. 8023, revised 1978) (26). Female BALB/c nude mice (age, 4 weeks; weight, 20 $\pm$ 5 g) and ZR751 cells were used for tumor xenograft experiments. All mice were maintained under controlled temperature (22 $\pm$ 1°C) and humidity (50 $\pm$ 5%) in a 12/12-h light/dark cycle with food and water available *ad libitum*. ZR751 cells transduced with different constructs (shDCXR-1 and shNC) were resuspended in PBS and injected subcutaneously into the armpits of nude mice (5 $\times$ 10<sup>6</sup> cells/100  $\mu$ l; 200  $\mu$ l). A total of 12 mice were randomly divided into two groups as follows: shNC (mice injected subcutaneously with ZR751 cells transduced

with shNC) and shDCXR (mice injected subcutaneously with ZR751 cells transduced with shDCXR-1). Tumors were measured weekly and the tumor volume (V) was calculated as follows:  $V = (\text{length} \times \text{width} \times 2) / 2$ . After 33 days, mice were anesthetized using 1% pentobarbital sodium (40 mg/kg) injected intraperitoneally and sacrificed by acute exsanguination after they became unconscious. The tumors were excised for IHC staining.

**Statistical analysis.** Experimental data are presented as the mean  $\pm$  standard error of the mean of a minimum of three independent experiments. GraphPad Prism 8 (GraphPad Software, Inc.) was used for statistical analysis. Unpaired Student's t test was used for comparisons between two groups, and paired Student's t-test was used to determine the statistical significance of differences in the expression levels in clinical tissue samples. In addition,  $\chi^2$  analysis was performed to assess the association of DCXR expression with tumor size, tumor stage, AJCC stage, distant metastasis and ER/PR/HER2-status. Univariate and multivariate Cox regression analysis were used to evaluate prognostic significance. Survival rate was analyzed by Kaplan-Meier with log-rank test. To test statistical significance between multiple groups, one-way ANOVA followed with Tukey's post hoc test was used. All statistical tests were two-sided.  $P < 0.05$  was considered to indicate a statistically significant difference.

## Results

**DCXR is upregulated and associated with tumor progression in human breast cancer tissue.** DCXR expression was assessed in 1,104 breast cancer and 113 paracancerous tissue samples from TCGA database. The results showed that DCXR was significantly upregulated in breast cancer tissue (Fig. 1A). A total of 80 patients' samples and data were collected for univariate and multivariate risk factor analysis and 30 patients were selected for RNA and protein expression verification; the expression levels of DCXR in the 50 patients were determined by IHC. RT-qPCR results showed that DCXR was significantly upregulated in breast cancer tissue compared with the paracancerous tissue (Fig. 1B). Furthermore, positive DCXR protein expression in breast cancer tissue was detected in 30 tissue samples by IHC staining. Subsequently, 30 patients were grouped into low- and high-expression populations according to the IHC score: 0-3 was defined as low protein expression and 4-9 was defined as high protein expression of DCXR (Fig. 1C). To determine the association between DCXR expression and breast cancer progression, the protein expression and clinical characteristics of 30 patients were picked at random to analyze. Survival rate, which was analyzed by Kaplan-Meier with log-rank test, showed that high expression of DCXR was associated with poor prognosis in patients with breast cancer (Fig. 1D). The  $\chi^2$  analysis of DCXR expression and tumor indicators suggested that high protein expression was associated with tumor size, tumor stage, American Joint Committee on Cancer (AJCC) stage, ER/PR/HER2-status and distant metastasis (Table I). Univariate regression analysis showed that DCXR expression, tumor size, tumor stage, AJCC stage and distant metastasis were significant predictors for breast cancer (Fig. 1E), whereas multivariate regression analysis further



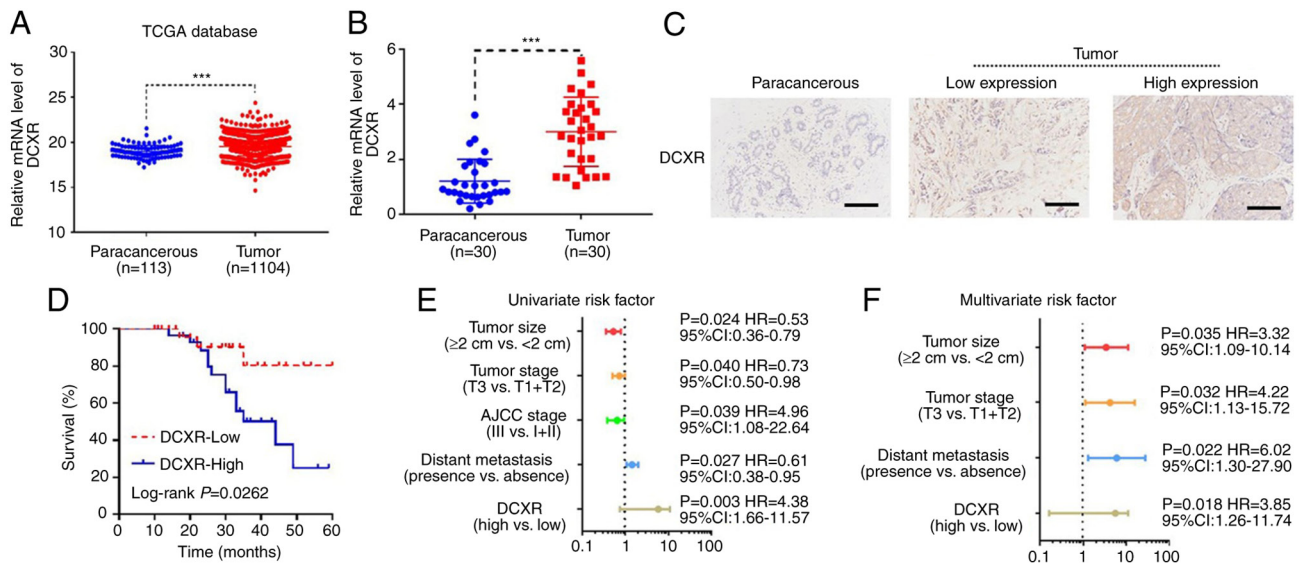


Figure 1. DCXR is upregulated and associated with cancer progression in human breast cancer tissue. (A) DCXR expression levels were increased in 1,104 human breast cancer compared with 113 paracancerous samples in TCGA database. (B) DCXR mRNA expression levels were determined using reverse transcription-quantitative PCR in 30 pairs of breast cancer and paracancerous tissue. The patients were grouped into low- and high-expression populations according to the immunohistochemistry score; 0-3 was defined as low protein expression and 4-9 was defined as high protein expression of DCXR. \*\*\* $P<0.001$ . (C) DCXR protein levels were examined using immunohistochemical staining assay in paracancerous and breast cancer tissue with low and high mRNA levels (scale bar, 200  $\mu$ m). (D) High expression of DCXR was associated with poor prognosis in patients with breast cancer. (E) Univariate and (F) multivariate risk factor analysis of DCXR expression, tumor size, tumor stage, AJCC stage and distant metastasis with breast cancer. AJCC, American Joint Committee on Cancer; DCXR, dicarbonyl/L-xylulose reductase; TCGA, The Cancer Genome Atlas.

demonstrated that, with the exception of AJCC stage, the other four risk factors were independent predictors of breast cancer aggressiveness, with significant HRs for predicting clinical outcome (Fig. 1F). These data indicated that upregulation of DCXR was associated with breast cancer progression.

*DCXR silencing suppresses proliferation, arrests the cell cycle and decreases glycolysis activity in human breast cancer cells.* GSEA showed that genes in the high-expression DCXR group were primarily enriched in 'glycolysis' and 'cell cycle' (Fig. 2A and B).

Next, *in vitro* experiments using breast cancer cell lines were used to assess the function of DCXR. DCXR mRNA and protein levels were upregulated in MDA-MB-231, BT-474, T47D, MCF-7 and ZR751 cells compared with MCF-10A normal human mammary epithelial cells (Fig. S1A and B). The two cell lines with the highest expression levels (ZR751 and BT-474) were selected for DCXR knockdown and MDA-MB-231, with the lowest expression, was selected for DCXR overexpression. DCXR was knocked down by transducing three different shDCXR into ZR751 and BT-474 cells; cells with shDCXR-1 and shDCXR-2 were selected for follow-up study based on the efficiency of shRNA; the results showed that all three shRNAs could effectively inhibit the expression of DCXR, and the shRNA with the best knockdown effect (shRNA-1) was selected for subsequent experiments (Fig. S1C and D). In shDCXR-1- and shDCXR-2-transduced ZR751 and BT-474 cells, proliferation was decreased at 24 and 48 h (Fig. 2C and E), cell cycle was arrested in G1 phase (Fig. 2E and F), the production of ATP and LD was decreased (Fig. 2G and H) and ECAR was decreased (Fig. 2I and J). These data suggested DCXR knockdown inhibited glycolysis and cell cycle of breast cancer cells.

*DCXR silencing suppresses tumorigenicity of human breast cancer cells in a mouse tumor model.* To identify the effect of DCXR on tumorigenicity of breast cancer cells, tumor growth was observed following injection of shDCXR- or shNC-transduced ZR751 cells into left flank of nude mice. At 33 days post-injection, DCXR interference was found to suppress the tumorigenic and proliferative ability of breast cancer cells; the volume of subcutaneous tumors was significantly smaller in the shDCXR group compared with the shNC group at 33 days post-injection (Fig. 3A and B). IHC assay for Ki-67 was used to assess cancer cell proliferation (23). The results showed that expression of Ki-67 was downregulated in tumor tissue of mice transplanted with DCXR-silenced cells by fluorescence staining (Fig. 3C), suggesting that DCXR silencing may suppress cell proliferation.

*Glycolysis inhibitor 2-DG abolishes the effect of DCXR on proliferation and glycolysis of human MDA-MB-231 cells.* The MDA-MB-231 cell line overexpressing DCXR was cultured to investigate the role of glycolysis inhibitor 2-DG on DCXR function in MDA-MB-231 breast cancer cells. Overexpression and knockdown of DCXR were detected by RT-qPCR and western blotting (Fig. S1C-F). DCXR overexpression promoted proliferation after 24 h (Fig. S2A), progression at S phase (Fig. S2B) and the production of ATP, LD and ECAR (Fig. S2C-E, respectively). 2-DG exposure for 24 and 48 h significantly inhibited cell proliferation, and its combination with DCXR overexpression suppressed oe-DCXR-induced cell proliferation (Fig. 4A). Subsequently, the role of 2-DG on DCXR-induced effects on cell cycle and glycolysis-associated indexes were evaluated. 2-DG exposure increased the number of MDA-MB-231 cells in G1 phase (Fig. 4B) and decreased production of ATP (Fig. 4C), LD (Fig. 4D) and ECAR (Fig. 4E),

Table I. Association between DCXR expression and clinicopathological characteristic in patients with breast cancer.

Clinicopathological characteristic	Number of cases	DCXR expression		P-value <sup>a</sup>
		High (%)	Low (%)	
Age, years				0.2007
≥50	32	14 (43.8)	18 (56.2)	
<50	48	28 (58.3)	20 (41.7)	
Tumor size, cm				0.0024
≥2	54	22 (40.7)	32 (59.3)	
<2	26	20 (76.92)	6 (23.08)	
Histopathology				0.2367
Ductal	55	32 (58.2)	23 (41.8)	
Lobular	25	18 (72.0)	7 (28.0)	
Histological grade				0.0317
1	13	3 (23.1)	10 (76.9)	
2	44	28 (63.6)	16 (36.4)	
3	23	11 (47.8)	12 (52.2)	
AJCC stage				0.0265
I	18	3 (16.7)	15 (83.3)	
II	20	12 (60)	8 (40)	
III	42	27 (64.3)	15 (35.7)	
Tumor stage				0.0382
T1	11	3 (27.3)	8 (72.7)	
T2	20	15 (66.7)	5 (33.3)	
T3	49	39 (33.3)	10 (66.7)	
Distant metastasis				0.0147
Presence	40	33 (82.5)	7(17.5)	
Absence	40	23 (57.5)	17 (42.5)	
ER status				0.0150
Positive	50	32 (62.7)	19 (37.3)	
Negative	30	10 (34.5)	19 (65.5)	
PR status				0.0015
Positive	54	35 (64.8)	19 (35.2)	
Negative	26	7 (26.9)	19 (73.1)	
HER2 status				0.0257
Positive	22	16 (72.7)	6 (27.3)	
Negative	58	26 (44.8)	32 (55.2)	

<sup>a</sup>Differences between groups were determined by  $\chi^2$  test. AJCC, American Joint Committee on Cancer; DCXR, dicarbonyl/L-xylulose reductase; ER, estrogen receptor; PR, progesterone receptor.

indicating that 2-DG suppressed the cell cycle and glycolytic metabolism. 2-DG treatment combined with oe-DCXR in MDA-MB-231 cells attenuated the effects of DCXR protein overexpression on the cell cycle, and glycolysis-associated indexes were also attenuated (Fig. 4A-E). These data indicated that the effect of DCXR on cell cycle progression and glycolysis was abrogated when glycolysis was inhibited.

## Discussion

To the best of our knowledge, the present study is the first to report an association between DCXR and disease progression

with respect to breast cancer. DCXR expression was upregulated and promoted cell cycle, proliferation and glycolytic metabolism in breast cancer.

DCXR was first noticed because of its association with pentosuria, a deficiency that elevates urine levels of L-xylulose (27). In addition to acting as a catalytic enzyme, DCXR performs other functions through protein-protein interactions, such as affecting sperm-zona pellucida interaction and cell adhesion (22,28). Its role in disease, such as infertility and cancer, has also been considered (18); however, our understanding of the role of DCXR in cancer is limited. In the present study, DCXR was highly expressed in breast

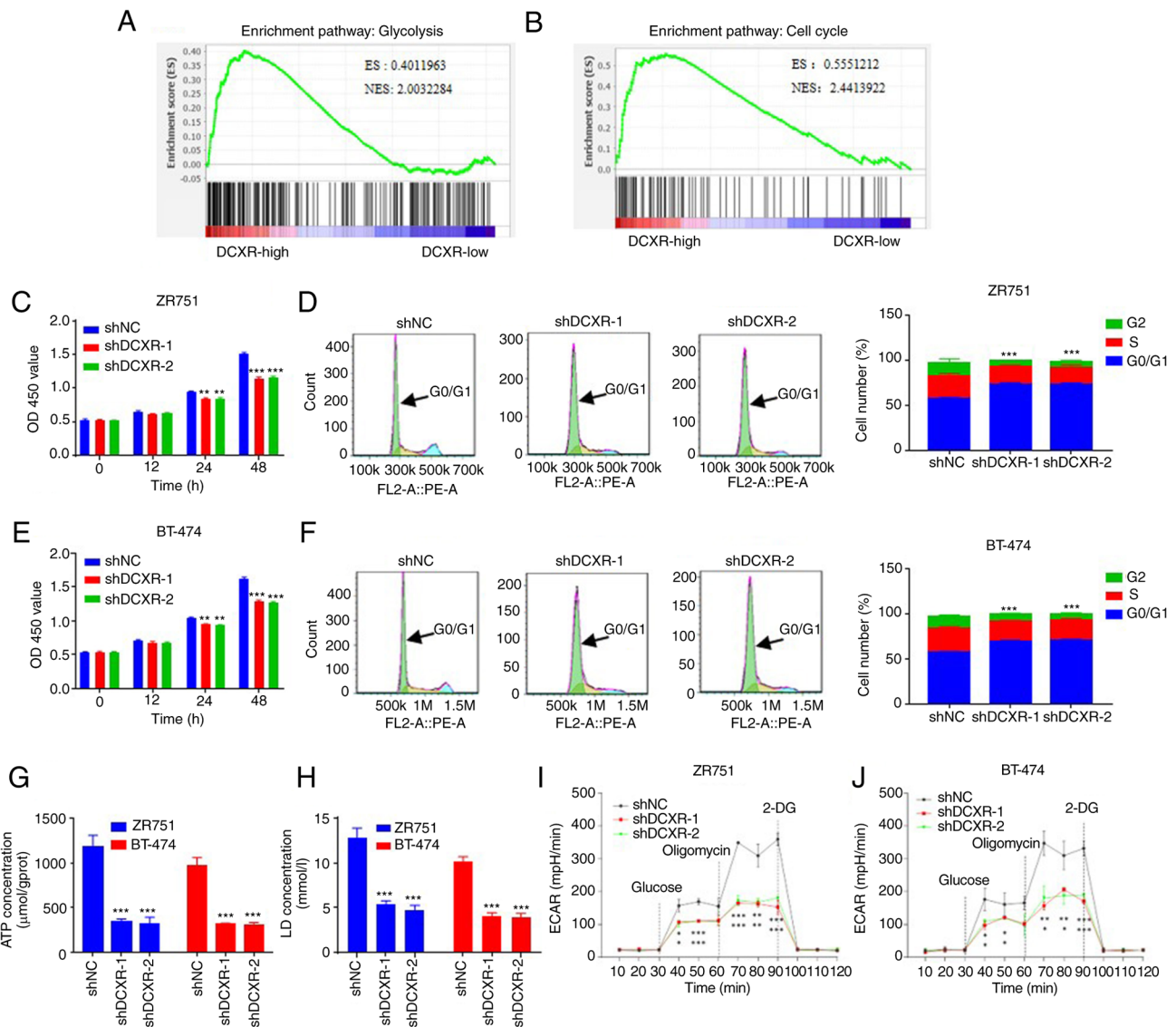


Figure 2. DCXR silencing suppresses proliferation, arrests the cell cycle and decreases glycolysis activity of human breast cancer cells. Bioinformatics analysis indicated that DCXR was enriched in (A) 'glycolysis' and (B) 'cell cycle' in breast cancer. Proliferation of (C) ZR751 and (D) BT-474 cells was suppressed following transduction with shDCXR-1 and shDCXR-2. Knockdown of DCXR arrested cells in G0/G1 phase in (E) ZR751 and (F) BT-474 cells. DCXR silencing decreased production of (G) ATP and (H) LD in ZR751 and BT-474 cells. Both shDCXR-1 and shDCXR-2 suppressed ECAR (mpH/min) in (I) ZR751 and (J) BT-474 cells. \* $P < 0.05$ , \*\* $P < 0.01$ , \*\*\* $P < 0.001$  vs. shNC. ES, enrichment Score; NES, normalized enrichment score; 2-DG, 2-deoxy-D-glucose; DCXR, dicarbonyl/L-xylulose reductase; ECAR, extracellular acidification rate; LD, lactate dehydrogenase; NC, negative control; OD, optical density; sh, short hairpin.

cancer tissue, based on the results of microarray assay from TCGA. Genome-wide gene expression analysis based on microarray technology is a key step in elucidating the molecular mechanisms of chronic disease, such as obesity, cardiovascular disease and cancer, and to identifying the key genes involved. The characteristic genes that discriminate healthy from unhealthy samples may be used as a target for drug development or as a molecular marker for diagnosis and prognosis (29). The present study results demonstrated DCXR expression levels were significantly higher in 30 clinical breast cancer samples compared with paracancerous tissue, which was consistent with results from TCGA. Thus, DCXR may be a molecular marker for breast cancer diagnosis. DCXR was subsequently associated with poor prognosis, tumor size, tumor stage, AJCC stage and distant metastasis. Overall, these results suggested that DCXR may serve as a potential

clinical diagnostic/prognostic marker and therapeutic target in breast cancer. Moreover, consistent with previously published articles, the presented data supported DCXR as an oncogene (18,19). The present study showed DCXR upregulation may be associated with breast cancer tumor progression and may be an independent risk factor for breast cancer.

The link between glycolysis and the cell cycle is important for cancer progression (30). The cell cycle is a process of cell division regulated by checkpoint controls; disrupted cell cycle underlies abnormal cell division and proliferation (31). Moreover, the cell cycle is an energy-intensive process, supported by oxidative phosphorylation and/or glycolysis (32). Cancer cells usually exhibit enhanced glycolysis that provides abundant ATP when necessary (for example at G1/S transition checkpoint) to support the proliferation and invasion of cancer cells (33,34). Certain studies have shown that signaling

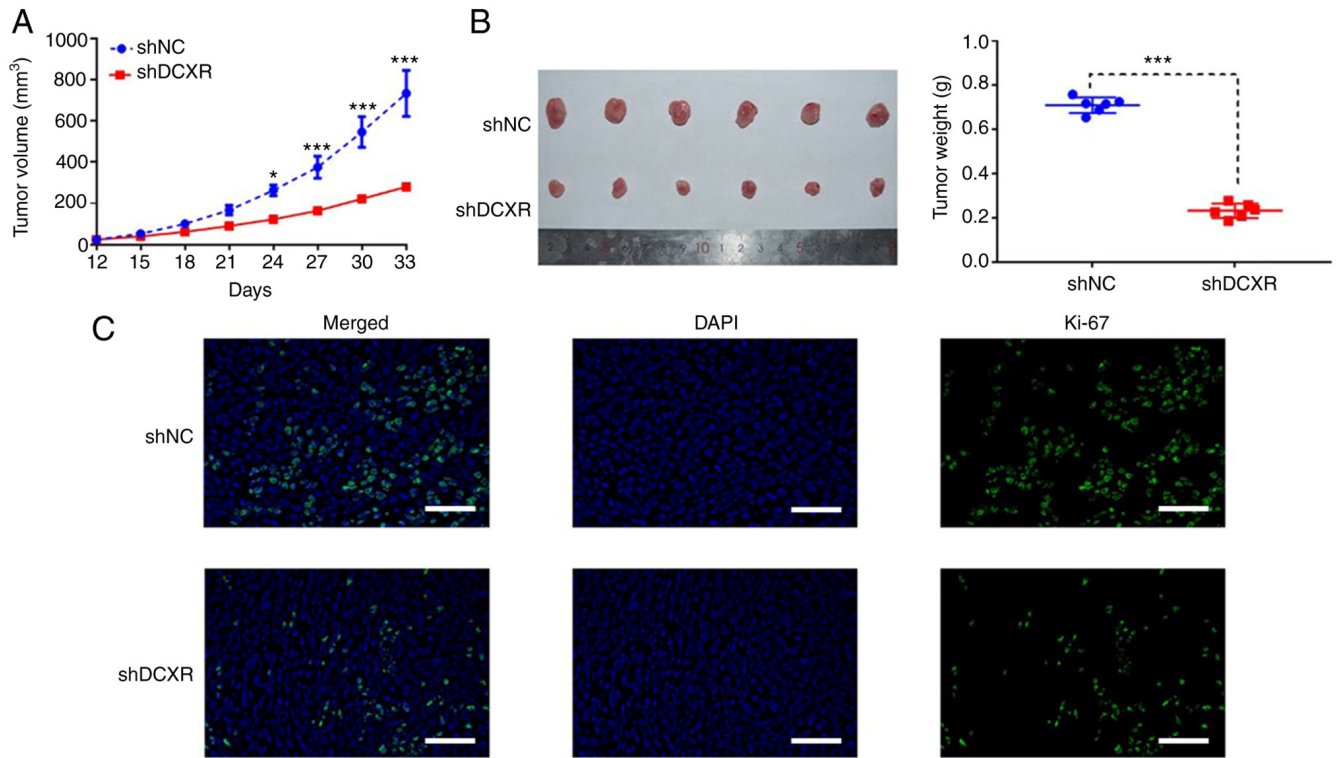


Figure 3. DCXR silencing suppresses tumorigenicity of human breast cancer cells in a mouse tumor model *in vivo*. Nude mice were subcutaneously injected with ZR751 cells transduced with shDCXR or shNC. Following injection, tumor (A) volume and (B) weight were measured; \*P<0.05, \*\*\*P<0.001 vs. shNC. (C) After 33 days of tumor growth, xenografts were removed for Ki-67 immunohistochemical staining to evaluate cell proliferation (scale bar, 200  $\mu$ m). DCXR, dicarbonyl/L-xylulose reductase; NC, negative control; sh, short hairpin RNA.

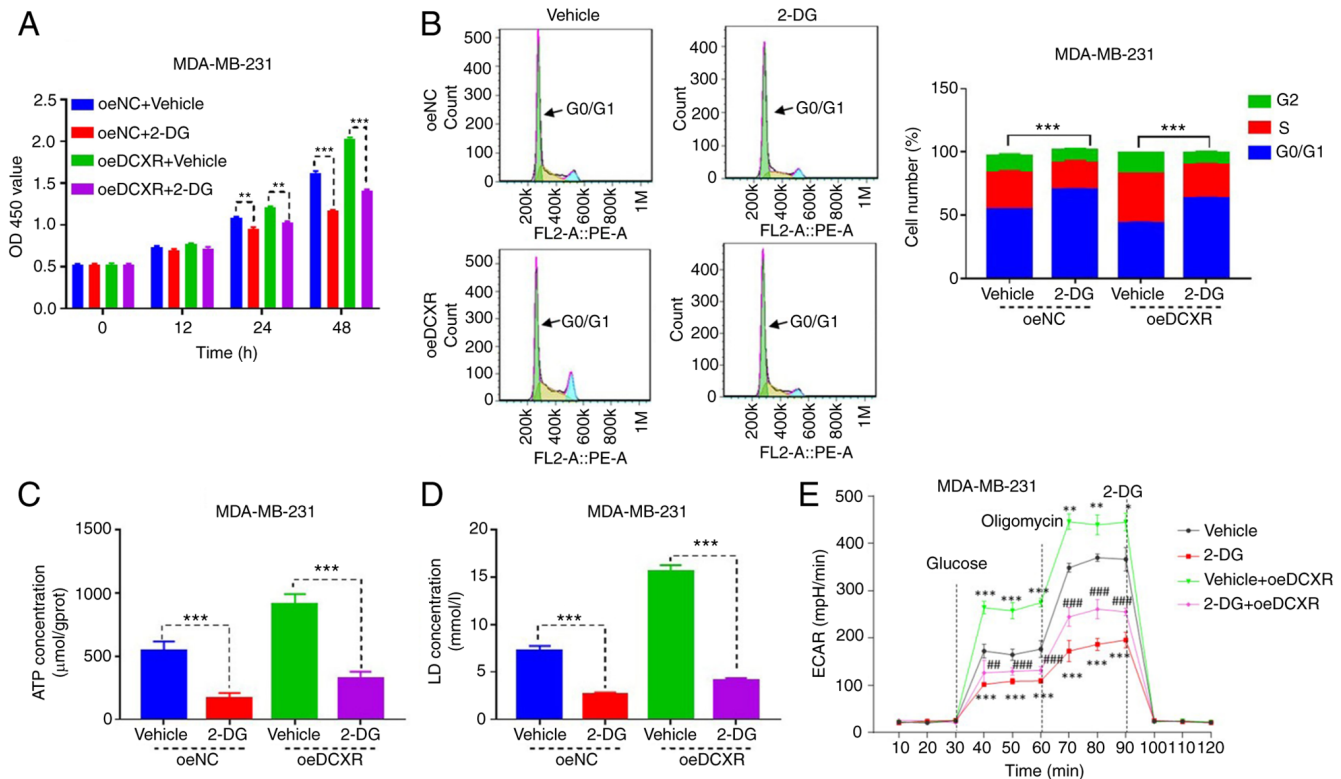


Figure 4. Glycolysis inhibitor 2-DG abolishes the effect of DCXR overexpression on proliferation and glycolytic metabolism of human MDA-MB-231 cells. (A) oeDCXR-transduced MDA-MB-231 breast cancer cells exhibited decreased cell proliferation in the presence of 2-DG. (B) 2-DG abolished the effect of oeDCXR on promoting the cycle of MDA-MB-231 cells. 2-DG exposure inhibited the production of (C) ATP and (D) LD in oeNC and oeDCXR-transduced cells. (E) ECAR (mpH/min) of oeDCXR-transduced cells was suppressed in the presence of the inhibitor 2-DG. \*\*\*P<0.001 vs. vehicle; ##P<0.01, ###P<0.001 vs. Vehicle + oeDCXR. 2-DG, 2-deoxy-D-glucose; DCXR, dicarbonyl/L-xylulose reductase; ECAR, extracellular acidification rate; LD, lactate dehydrogenase; NC, negative control; OD, optical density; oe, overexpression.



molecules critical for glycolysis regulate breast cancer cell proliferation (11,35-37). To the best of our knowledge, however, the function of DCXR in cell events and glycolytic metabolism during disease progression has been rarely studied. The present study investigated the role of DCXR in regulating glycolysis and cell cycle in breast cancer cells because the function of DCXR was significantly enriched in 'glycolysis', as indicated by GSEA bioinformatics analysis. DCXR loss- or gain-of-function results suggested that DCXR silencing inhibited both glycolysis and cell cycle G1/S checkpoint progression, whereas DCXR overexpression promoted glycolysis and G1/S phase progression. To the best of our knowledge, this is the first study demonstrating that DCXR promotes glycolytic metabolism. Therefore, we hypothesized that DCXR may promote breast cancer development by regulating glycolysis and cell cycle. This phenomenon was further supported by *in vivo* experiments using mice with xenograft tumors, which showed that DCXR silencing limited tumor growth and proliferation; *in vitro* human breast cancer cell assays showed that exposure to glycolysis inhibitor 2-DG abolished the promoting effect of DCXR overexpression on cell cycle and glycolysis. Previous studies have shown that the function of DCXR is enzyme catalysis and protein-protein interaction-mediated cell adhesion in cancer cells (19,20). The present study demonstrated a novel function of DCXR in enhancing glycolytic metabolism and promoting proliferation of breast cancer cells. The present study had certain limitations. First, the reason for the increase in DCXR has not been identified. Furthermore, the molecular mechanism of glucose metabolism in animals has not been clarified. These will be the focus of future research.

The present findings suggested that DCXR may be an oncogene in breast cancer cells and may be associated with tumor progression. These results revealed that DCXR may regulate glycolysis, cell cycle progression and proliferation in breast cancer cells. This study investigated the biological function of DCXR and provided a basis for the application of DCXR as a marker or therapeutic target for breast cancer.

### Acknowledgements

Not applicable.

### Funding

The present study was supported by The Scientific Research Project of Shanghai Municipal Health Commission (grant no. 201940502) and The Science and Technology Development Fund of Shanghai Pudong New Area (grant no. PKJ2019-Y14).

### Availability of data and materials

All data generated or analyzed during the present study are included in this published article.

### Authors' contributions

YY and BZ contributed to the conception and design of this study. YJ and MZ performed the experiments, collected the data and performed statistical analysis with the help of YT and

LQ. YJ and MZ drafted the manuscript, which was corrected and revised by YY and BZ. YY, BZ, YJ and MZ confirm the authenticity of all the raw data. All authors read and approved the final manuscript.

### Ethics approval and consent to participate

Written informed consent was obtained from all patients and research protocols were approved by the Ethics Committee of Shanghai Seventh's People's Hospital (approval no. 2020-7th-H IRB-031). All experimental procedures involving animals were approved by The Animal Care and Use Committee of Shanghai Seventh's People's Hospital (approval no. 2021-AR-011).

### Patient consent for publication

Not applicable.

### Competing interests

The authors declare that they have no competing interests.

### References

1. Sung H, Ferlay J, Siegel RL, Laversanne M, Soerjomataram I, Jemal A and Bray F: Global cancer statistics 2020: GLOBOCAN estimates of incidence and mortality worldwide for 36 cancers in 185 countries. *CA Cancer J Clin* 71: 209-249, 2021.
2. Solanki M and Visscher D: Pathology of breast cancer in the last half century. *Hum Pathol* 95: 137-148, 2020.
3. Wang HX and Gires O: Tumor-derived extracellular vesicles in breast cancer: From bench to bedside. *Cancer Lett* 460: 54-64, 2019.
4. Tsang JYS and Tse GM: Molecular classification of breast cancer. *Adv Anat Pathol* 27: 27-35, 2020.
5. Kandel A, Dhillon SK, Prabakaran CB, Hisham SFB, Rajamanickam K, Napper S, Chidambaram SB, Essa MM, Yang J and Sakharkar MK: Identifying kinase targets of PPARgamma in human breast cancer. *J Drug Target* 29: 660-668, 2021.
6. Rossi FA, Steinberg JH, Roitberg EH, Joshi MU, Pandey A, Abba MC, Dufresne B, Buglioni S, Laurenzi VD, Sala G, *et al*: USP19 modulates cancer cell migration and invasion and acts as a novel prognostic marker in patients with early breast cancer. *Oncogenesis* 10: 28, 2021.
7. Wang YP and Lei QY: Perspectives of reprogramming breast cancer metabolism. *Adv Exp Med Biol* 1026: 217-232, 2017.
8. Wu Z, Wu J, Zhao Q, Fu S and Jin J: Emerging roles of aerobic glycolysis in breast cancer. *Clin Transl Oncol* 22: 631-646, 2020.
9. Heiden MG, Cantley LC and Thompson CB: Understanding the Warburg effect: The metabolic requirements of cell proliferation. *Science* 324: 1029-1033, 2009.
10. Vaupel P, Schmidberger H and Mayer A: The Warburg effect: Essential part of metabolic reprogramming and central contributor to cancer progression. *Int J Radiat Biol* 95: 912-919, 2019.
11. Enzo E, Santinon G, Pocaterra A, Aragona M, Bresolin S, Forcato M, Grifoni D, Pession A, Zanconato F, Guzzo G, *et al*: Aerobic glycolysis tunes YAP/TAZ transcriptional activity. *EMBO J* 34: 1349-1370, 2015.
12. Zhao Y, He J, Yang L, Luo Q and Liu Z: Histone deacetylase-3 modification of MicroRNA-31 promotes cell proliferation and aerobic glycolysis in breast cancer and is predictive of poor prognosis. *J Breast Cancer* 21: 112-123, 2018.
13. Zhang HS, Du GY, Zhang ZG, Zhou Z, Sun HL, Yu XY, Shi YT, Xiong DN, Li H and Huang YH: NRF2 facilitates breast cancer cell growth via HIF1a-mediated metabolic reprogramming. *Int J Biochem Cell Biol* 95: 85-92, 2018.
14. van Weverwijk A, Koundouros N, Iravani M, Ashenden M, Gao Q, Poulgiannis G, Jungwirth U and Isacke CM: Metabolic adaptability in metastatic breast cancer by AKR1B10-dependent balancing of glycolysis and fatty acid oxidation. *Nat Commun* 10: 2698, 2019.

15. Perco P, Ju W, Kerschbaum J, Leierer J, Menon R, Zhu C, Kretzler M, Mayer G, Rudnicki M and Nephrotic Syndrome Study Network (NEPTUNE): Identification of dicarbonyl and L-xylulose reductase as a therapeutic target in human chronic kidney disease. *JCI Insight* 4: e128120, 2019.
16. Hu XH, Ding LY, Huang WX, Yang XM, Xie F, Xu M and Yu L: (-)-Epigallocatechin-3-gallate, a potential inhibitor to human dicarbonyl/L-xylulose reductase. *J Biochem* 154: 167-175; 2013.
17. Yang S, Jan YH, Mishin V, Heck DE, Laskin DL and Laskin JD: Diacetyl/l-xylulose reductase mediates chemical redox cycling in lung epithelial cells. *Chem Res Toxicol* 30: 1406-1418, 2017.
18. Ebert B, Kisiela M and Maser E: Human DCXR-another 'moonlighting protein' involved in sugar metabolism, carbonyl detoxification, cell adhesion and male fertility? *Biol Rev Camb Philos Soc* 90: 254-278, 2015.
19. Jeffery CJ: Moonlighting proteins: Old proteins learning new tricks. *Trends Genet* 19: 415-417, 2003.
20. Cho-Vega JH, Tsavachidis S, Do KA, Nakagawa J, Medeiros LJ and McDonnell TJ: Dicarbonyl/L-xylulose reductase: A potential biomarker identified by laser-capture microdissection-microserial analysis of gene expression of human prostate adenocarcinoma. *Cancer Epidemiol Biomarkers Prev* 16: 2615-2622, 2007.
21. Lee SK, Son LT, Choi HJ and Ahnn J: Dicarbonyl/l-xylulose reductase (DCXR): The multifunctional pentosuria enzyme. *Int J Biochem Cell Biol* 45: 2563-2567, 2013.
22. Cho-Vega JH, Vega F, Schwartz MR and Prieto VG: Expression of dicarbonyl/L-xylulose reductase (DCXR) in human skin and melanocytic lesions: morphological studies supporting cell adhesion function of DCXR. *J Cutan Pathol* 34: 535-542, 2007.
23. Hang X, Wu Z, Chu K, Yu G, Peng H, Xin H, Miao X, Wang J and Xu W: Low expression of DCXR protein indicates a poor prognosis for hepatocellular carcinoma patients. *Tumour Biol* 37: 15079-15085, 2016.
24. Xu J, Qin S, Yi Y, Gao H, Liu X, Ma F and Guan M: Delving into the heterogeneity of different breast cancer subtypes and the prognostic models utilizing scRNA-Seq and Bulk RNA-Seq. *Int J Mol Sci* 23: 9936, 2022.
25. Livak KJ and Schmittgen TD: Analysis of relative gene expression data using real-time quantitative PCR and the 2(-Delta Delta C(T)) method. *Methods* 25: 402-408, 2001.
26. Shi B, Xue M, Wang Y, Wang Y, Li D, Zhao X and Li X: An improved method for increasing the efficiency of gene transfection and transduction. *Int J Physiol Pathophysiol Pharmacol* 10: 95-104, 2013.
27. National Research Council (US) Committee for the Update of the Guide for the Care and Use of Laboratory Animals. *Guide for the Care and Use of Laboratory Animals*. 8th ed. Washington (DC): National Academies Press (US); 2011.
28. Penault-Llorca F and Radosevich-Robin N: Ki67 assessment in breast cancer: An update. *Pathology* 49: 166-171, 2017.
29. Kim YN, Kim SH, Son LT, Ahnn J and Lee SK: Dicarbonyl/L-xylulose reductase (DCXR) producing xylitol regulates egg retention through osmolality control in *Caenorhabditis elegans*. *Anim Cells Syst (Seoul)* 26: 223-231, 2013.
30. Moskovtsev SI, Jarvi K, Legare C, Sullivan R and Mullen JB: Epididymal P34H protein deficiency in men evaluated for infertility. *Fertil Steril* 88: 1455-1457, 2007.
31. Kim K, Zakharkin SO and Allison DB: Expectations, validity, and reality in gene expression profiling. *J Clin Epidemiol* 63: 950-959, 2010.
32. Icard P, Fournel L, Wu Z, Alifano M and Lincet H: Interconnection between metabolism and cell cycle in cancer. *Trends Biochem Sci* 44: 490-501, 2019.
33. Williams GH and Stoeber K: The cell cycle and cancer. *J Pathol* 226: 352-364, 2012.
34. Salazar-Roa M and Malumbres M: Fueling the cell division cycle. *Trends Cell Biol* 27: 69-81, 2017.
35. Abbaszadeh Z, Cesmeli S and Avci CB: Crucial players in glycolysis: Cancer progress. *Gene* 726: 144158, 2020.
36. Li L, Liang Y, Kang L, Liu Y, Gao S, Chen S, Li Y, You W, Dong Q, Hong T, *et al*: Transcriptional regulation of the warburg effect in cancer by SIX1. *Cancer Cell* 33: 368-385 e367, 2018.
37. Qiao L, Dong C and Ma B: UBE2T promotes proliferation, invasion and glycolysis of breast cancer cells by regulating the PI3K/AKT signaling pathway. *J Recept Signal Transduct Res* 42: 151-159, 2021.



This work is licensed under a Creative Commons Attribution-NonCommercial-NoDerivatives 4.0 International (CC BY-NC-ND 4.0) License.